Accepted version

Pedro J. Lee, John P. Vtkovsk, Martin F. Lambert, Angus R. Simpson and James A. Liggett
Frequency domain analysis for detecting pipeline leaks
Journal of Hydraulic Engineering, 2005; 131(7):596-604

http://doi.org/10.1061/(ASCE)0733-9429(2005)131:7(596)

Frequency domain analysis for detecting pipeline leaks

by

Lee, P.J., Vítkovský, J.P., Lambert, M.F., Simpson, A.R. and Liggett, J.A.

Journal of Hydraulic Engineering

Citation:
Lee, P.J., Vítkovský, J.P., Lambert, M.F., Simpson, A.R. and Liggett, J.A. (2005). "Frequency domain analysis for detecting pipeline leaks." *Journal of Hydraulic Engineering*, American Society of Civil Engineers, Vol. 131, No. 7, July, 596–604 (41 citations to Jan. 2013 – Scopus)

Detection of Leaks in Fluid Pipelines Using a Linear System Transfer Function

Pedro J. Lee[1], John P. Vítkovský[2], Martin F. Lambert[3], Angus R. Simpson[4], and James A. Liggett[5]

Keywords: Leakage, Water Pipelines, Frequency response, Random vibration, Monitoring, Resonance, Transfer functions, Transient flow, Linear systems

ABSTRACT: This paper introduces leak detection methods that involve the injection of a continuous fluid transient into the pipeline, creating a time-invariant system that is analyzed in the frequency domain. This method of analysis moves away from the conventional time-domain approach of fluid transients into an area where information concerning the leak is extracted from the frequency behavior of the pipeline system. Two methods of leak detection using the frequency response of the pipeline are proposed, along with the practical application of these methods in a realistic situation. The two leak detection methods are the inverse resonance method and the resonance peak-sequencing method. The use of pseudo-random binary signals for the generation of the frequency response of a single pipeline system can increase the signal to noise ratio of the data and allow efficient extraction of the frequency response information. The measurement position has been found to affect the shape of the frequency response diagram. As a result, the optimum measurement position for pipelines with asymmetric boundary conditions was determined. Preliminary numerical testing has found both techniques able to detect and locate a leak in a single pipeline configuration.

[1] Postgraduate Student, Department of Civil & Environmental Engineering, The University of Adelaide, Adelaide SA 5005, Australia; Phone: +61 8 8303 5134; Fax: +61 8 8303 4359; Email: plee@civeng.adelaide.edu.au

[2] Research Associate, Department of Civil & Environmental Engineering, The University of Adelaide, Adelaide SA 5005, Australia; Phone: +61 8 8303 4324; Fax: +61 8 8303 4359; Email: jvitkovs@civeng.adelaide.edu.au

[3] Senior Lecturer, Department of Civil & Environmental Engineering, The University of Adelaide, Adelaide SA 5005, Australia; Phone: +61 8 8303 5838; Fax: +61 8 8303 4359; Email: mlambert@civeng.adelaide.edu.au

[4] Associate Professor, Department of Civil & Environmental Engineering, The University of Adelaide, Adelaide SA 5005, Australia; Phone: +61 8 8303 5874; Fax: +61 8 8303 4359; Email: asimpson@civeng.adelaide.edu.au

[5] Professor Emeritus, School of Civil & Environmental Engineering, Cornell University, Ithaca, NY 14853-3501, USA. Email: jal8@cornell.edu

INTRODUCTION

Fluid transients in pipes—water hammer waves—are changed by pipeline properties, including leaks and blockages, thus leaving clues to such properties. Analysis of transients can reveal a substantial amount of information concerning the integrity of the system. Numerous methods utilize transient behavior for the purpose of leak detection. These include the inverse transient method (Liggett and Chen 1994, Liou *et al.* 1995, Vítkovský and Simpson 1997, Nash and Karney 1999, Vítkovský *et al.* 1999, Tang *et al*. 2000, Vítkovský *et al*. 2001), the transient damping method (Wang, *et al.* 2002), and time-domain reflectometry techniques (Jönsson and Larson 1992, Brunone 1999, Covas and Ramos 1999, Lee *et al.* 2002).

This paper proposes the use of a generated time-invariant signal as a means of leak detection and signal-processing techniques provide a means of analysing these signals in the frequency domain.

The concepts of steady oscillatory flow and pipeline resonance are well established, and details can be found in Zielke *et al.* (1969, 1971), Chaudhry (1970, 1987), Fox (1977), and Wylie *et al.* (1993). Similar to other mechanical systems, the magnitude of a system response is frequency dependent. While a pipeline reinforces and transmits input signals of a particular frequency (for example, the fundamental frequency), others are effectively absorbed within the system. Thus, pipeline systems are similar to frequency filters, the characteristics of which are determined by system properties such as boundary conditions, friction, and wave speed.

The degree that each frequency component is absorbed or transmitted within the pipeline is defined by a frequency response diagram (FRD), also known as the transfer function for the system (Lynn, 1982). This diagram relates both the magnitude and phase of the system output to the system input for different frequencies. The FRD is uniquely defined from the output when driven with a broadband input signal that has a unit magnitude for all frequencies.

The medical field was amongst the first to use the FRD of pipe-like systems for the measurement in the human vocal tract (Schoeder 1967, Mermelstein 1967). Schoeder (1967) found that localized changes in the area of the tract impose shifts in the resonance peaks of the FRD, and Mermelstein (1967) provided numerical verification of this finding. Antonopoulos-Domis (1980), Qunli and Fricke (1989), Qunli and Fricke (1991), and De Salis

and Oldham (1999, 2001) further improved the method and applied it extensively to the detection and location of blockages in gas pipelines.

Recently such ideas have been applied in the field of leak detection. Mpesha (1999), Mpesha *et al.* (2001, 2002) suggested that the presence of leaks and other features within a pipeline system induce the formation of new resonance peaks within the frequency response function. However, doubt about the method of Mpesha, *et al.* (2001, 2002) has been expressed in a discussion of the paper by Lee *et al.* (2002a).

A transfer function—describing the relationship between the frequency spectrums at the input and the output—can be generated using linear systems theory (Lynn 1982; Liou 1998; De Salis and Oldham 1999, 2001). A wide-band signal fed into the system while measuring the output, generates the response at a wide range of frequencies simultaneously. When a pipeline system is excited by such a signal, the frequency response function is related to the Fourier spectrum of the input and output signals by

$$H(\omega) = \frac{Y(\omega)}{X(\omega)} \tag{1}$$

where, $X(\omega)$ and $Y(\omega)$ = Fourier transforms of the input and output signal respectively, and $H(\omega)$ = frequency response function of the linear system.

The ratio between the Fourier spectrum of the output and input signals yields a function that describes the magnification and phase change (i.e., the frequency response function) of each frequency component contained within the input. The system response is efficiently calculated using a pseudo-random binary signal or other wide band signal as the system input in a single application of Eq. (1).

Wylie *et al.* (1993) and Ferrante *et al.* (2001) used the impedance equations to generate the transfer function for single pipeline systems. The transfer function generated by the impedance equations describes the ratio between the frequency spectrum—expressed as a complex number—of the complex discharge and complex head at a point in the pipeline, defined as the hydraulic impedance of that point. However, a problem associated with this definition of the transfer function is that discharge is difficult to measure accurately under transient conditions

and does not lend itself to input-output methodologies that are consistent with existing signal processing and system analysis theories.

Ferrante *et al.* (2001) indicated that the location of a leak affects the relative magnitude of the resonance peaks in the transfer function, but the impact of a leak on the location of resonance frequencies is minimal, except in the case of large leaks (contrasting with the effect of blockages, which do influence the location of resonance frequencies). This finding leads to a proposed method that uses the relative sizes of resonance peaks of different harmonics as a means of leak location in a single pipeline as explained below. The techniques of blockage detection proposed in Antonopoulos-Domis (1980), Qunli and Fricke (1989), Qunli and Fricke (1991), De Salis and Oldham (1999, 2001), which use resonant peak shifts, are not directly applicable to leak detection.

This paper uses time-invariant perturbation of flow generated by an in-line valve that flutters in a specified pattern. An upstream reservoir and a fluctuating downstream valve discharging into a constant head reservoir bound the pipeline. An illustration of the pipeline configuration is shown in Figure 1. Two methods of leak detection are proposed in this paper. An inverse calibration scheme forms the basis one of the method. In addition, a method for accurately locating the position of a leak within the pipeline using a resonance peak-sequencing method is also introduced. Both methods require the accurate determination of the FRD. A discussion of pseudo-random binary signals and how they can be used to provide an efficient estimate of the FRD under realistic conditions forms the final part of the paper.

BACKGROUND

The impedance method (Fox, 1989, Wylie *et al.* 1993, Ferrante *et al.* 2001) and the transfer matrix method (Chaudhry 1970, 1987) make use of linearized forms of the momentum and continuity equations in the frequency domain, and are well suited to purely sinusoidal oscillatory flow situations. The impedance method, however, is mathematically complex and requires the calculation of the "hydraulic impedance," defined as the ratio between the complex oscillatory head and the discharge at a point within the pipeline. The incorporation of system friction and other system components in the impedance equations complicates the analysis. In comparison, the transfer matrix method, which describes each pipeline component as a discrete matrix, is more elegant and flexible, and can be used to incorporate a high level of detail in the model without dramatically

increasing the complexity of the mathematics. For these reasons, the transfer matrix method is used in this paper.

The governing equations for unsteady flow in a closed conduit are the conservation of mass and linear-momentum equations, given by Eqs. (2) and (3) respectively (Wylie *et al.*, 1993)

$$\frac{\partial Q}{\partial x} + \frac{gA}{a^2}\frac{\partial H}{\partial t} = 0 \tag{2}$$

$$\frac{\partial H}{\partial x} + \frac{1}{gA}\frac{\partial Q}{\partial t} + \frac{fQ|Q|}{2gDA^2} = 0 \tag{3}$$

where, Q and H = discharge and head in the pipe respectively, g = gravitational acceleration, D = pipe diameter, A = pipe cross-sectional area, a = wave speed, f = Darcy-Weisbach friction factor, x = distance along the pipe and t = time.

In the case of steady oscillatory flow, the discharge and head can be equated to the sum of a mean and a sinusoidal oscillatory component,

$$Q = Q_0 + q^* \tag{4}$$

$$H = H_0 + h^* \tag{5}$$

$$q^* = \mathrm{Re}(q(x)e^{i\omega t}) \tag{6}$$

$$h^* = \mathrm{Re}(h(x)e^{i\omega t}) \tag{7}$$

where, Q_0, H_0 = mean discharge and head at a point within the pipe. q^*, h^* = oscillatory components, and q, h = magnitude of the oscillations, and are complex functions of the position with the pipe, x. Re(z) represents the

real part of the arbitrary variable z, while $e^{i\omega t}$ describes the sinusoidal oscillation of the frequency ω, with $i = \sqrt{-1}$.

Substitution of Eqs. (4) and (5) into Eqs. (2) and (3) and subsequent linearization of the frictional term produces

$$\frac{dq}{dx} + \frac{gA\omega i}{a^2} h = 0 \tag{8}$$

$$\frac{dh}{dx} + \left(\frac{\omega i}{gA} + R \right) q = 0 \tag{9}$$

where, R = the frictional resistance term, equal to $(fQ_0)/(gDA^2)$ for turbulent flows or$(32\upsilon)/(gAD^2)$ for laminar flows. Note that the sinusoidal oscillation variables q^* and h^* are replaced by the complex magnitude variables q and h by canceling the common exponential term from each equation.

Eqs. (8) and (9) represent a set of ordinary differential equations that are solved using separation of variables. The solution is expressed in matrix form relating the magnitude of the discharge and head fluctuation in the upstream and downstream ends of the pipe segment,

$$\begin{Bmatrix} q \\ h \end{Bmatrix}^{n+1} = \begin{bmatrix} \cosh \mu_k l_k & -\frac{1}{Z_k} \sinh \mu_k l_k \\ -Z_k \sinh \mu_k l_k & \cosh \mu_k l_k \end{bmatrix} \begin{Bmatrix} q \\ h \end{Bmatrix}^{n} \tag{10}$$

where $Z_k = \frac{\mu_k a_k^2}{i\omega g A_k}$ (the characteristic impedance for the k^{th} pipe section), and superscripts n and subscript k denotes the node and link number within the system respectively in which the link k lies between the upstream node n and downstream node $n + 1$. The propagation function is $\mu = \frac{1}{a}\sqrt{-\omega^2 + igA\omega R}$, and l_k is the length of the uniform pipe section under consideration.

Linearizations used to create Eq. (10) are valid if abs(q) << $|Q_0|$ for $Q_0 \neq 0$, abs(h) << $|\Delta H|$ where ΔH is the difference in head at the extremities of the pipeline, $\text{abs}(P) = \sqrt{P_r^2 + P_i^2}$ denoting the absolute value of an arbitrary imaginary number P.

Similar matrices can be derived for different link components within the pipeline. The problem considered herein considers the impact of a leak on the frequency response diagram of a single pipeline system bounded by an upstream reservoir and a downstream valve. Oscillating the valve opening provides the excitation of the system. The valve orifice equation relating the head loss across the valve to the flow through the valve is

$$Q_V = C_V \tau \sqrt{\Delta H_V} \tag{11}$$

where Q_V = flow through the valve, ΔH_V = difference in head across the valve, C_V = valve coefficient and τ = dimensionless valve opening = $\frac{C_d A_V}{(C_d A_V)_{\text{Ref}}}$ where the subscript 'Ref' refers to a reference valve opening size at steady state and A_V = area of the valve aperture.

Substitution of $\tau = \tau_0 + \text{Re}(\Delta\tau e^{i\omega t})$, and Eq. (4), Eq. (5) into Eq. (11) followed by linearization gives

$$\begin{Bmatrix} q \\ h \end{Bmatrix}^{n+1} = \begin{bmatrix} 1 & 0 \\ -\frac{2\Delta H_{V0}}{Q_{V0}} & 1 \end{bmatrix} \begin{Bmatrix} q \\ h \end{Bmatrix}^{n} + \begin{bmatrix} 0 \\ \frac{2\Delta H_{V0}\Delta\tau}{\tau_0} \end{bmatrix} \tag{12}$$

where, Q_{V0}, H_{V0} = steady state flow through the valve and the steady state head loss across the valve respectively and $\Delta\tau$ = complex variable describing the magnitude of the valve oscillation, τ_0 = dimensionless valve opening at steady state . Eq. (12) is first order accurate for small perturbations given that $\text{Re}(\Delta\tau e^{i\omega t}) << |\tau_0|$. As $\Delta\tau$ is real, $\text{Re}(\Delta\tau)$ is replaced by $\Delta\tau$ for the duration of this paper.

The discharge from the leak is expressed by the orifice equation,

$$Q_L = C_d A_L \sqrt{2gH_L} \tag{13}$$

where, C_dA_L = lumped discharge coefficient of the leak orifice and H_L = head at the leak orifice, and Q_L = discharge out of the leak orifice. Substituting Eqs. (4) and (5) into Eq. (13) and linearizing gives,

$$\begin{Bmatrix} q \\ h \end{Bmatrix}^{n+1} = \begin{bmatrix} 1 & -\dfrac{Q_{L0}}{2H_{L0}} \\ 0 & 1 \end{bmatrix} \begin{Bmatrix} q \\ h \end{Bmatrix}^{n} \tag{14}$$

where, Q_{L0}, H_{L0} = steady state flow out of the leak and steady state head at the leak respectively.

Notice that each transfer matrix determines the value of the head and discharge oscillation downstream by drawing upon information upstream. These transfer matrices can be combined by multiplication to form an overall transfer matrix for the entire pipeline system. Multiplication starts from the downstream and progresses upstream. The system can be solved once the boundary conditions are known (Chaudhry, 1987).

Due to the linearized nature of the transfer matrix equations, however, care must be taken so that the magnitude of the sinusoidal driving function does not exceed linearizing approximations. An alternative to the transfer matrix method for analyzing steady oscillatory flow is to use the method of characteristics, a time domain solution to the full nonlinear Eqs (2) and (3). While slower in comparison to the transfer matrix technique for analyzing steady oscillatory flow with sinusoidal inputs, the method of characteristics is a reliable transient analysis tool that has been used extensively in the development of other transient based leak detection methods. For the application of non-sinusoidal input signals the method of characteristics produces faster computer run times than the transfer matrices.

To illustrate the importance of operating within the bounds of the linearization assumption when using the transfer matrix equations, the method of characteristics was used to generate data for a simple reservoir-pipe-valve system. The valve oscillates with a fixed frequency. Calculations begin with steady flow and proceed until steady oscillatory flow is achieved.

Figure 2 shows a Fourier decomposition of the steady oscillatory portion of the time series data at an arbitrary forcing frequency of 9.76 ω_{th}, where ω_{th} is the fundamental frequency of the pipeline, defined as,

$$\omega_{th} = 4\sum_{k=1}^{n_{pipe}} \frac{L}{a} \tag{15}$$

where n_{pipe} = number of pipe sections in the system. Figure 2, generated by the MOC as described above, indicates that a valve perturbation magnitude of 0.10% of the original valve opening size, $\tau_{0,}$ results in an oscillation that contains only a single frequency, equal to the driving frequency at the valve. In comparison, when $\Delta\tau$ = 30% of the original valve opening, more than one frequency in the measured output is observed. The additional frequency components suggest that the system is nonlinear; that energy can travel between different frequencies. For such situations the use of the transfer matrix equations leads to inaccurate results.

Figure 3 illustrates the percentage linearization error as a function of the valve perturbation. The error is quantified using the difference between the power of the driving frequency component in the output and the total power of the sinusoidal input signal. The error grows exponentially and reaches a value of 1% at a $\Delta\tau/\tau_0$ of 0.15, and the value of $\Delta\tau/\tau_0$ = 0.3 used in Figure 2 gives an error of 4.3%.

PROPERTIES OF THE FREQUENCY RESPONSE DIAGRAM

Two important parameters that can change the FRD are the impact of both the measurement position and the presence of a leak within the pipeline. The system shown in Figure 1 is used to illustrate the impact of these fundamental parameters on the FRD of a simple pipeline system. The system parameters are shown in Table 1.

The magnitude of the valve perturbation is set such that linear approximation error is small while the output signal is large enough for accurate measurement. From Figure 3, the linearization error at $\Delta\tau/\tau_0$ = 0.1 is 0.6% while giving a 5-6 m range in the head. A smaller value of valve perturbation results in a lower linearization error, but also reduces the detectability of the transient response in a realistic situation.

The FRD describes the magnitude of the head perturbation observed at a point in the pipeline when the system is excited by different frequencies. In the case of a simple pipeline system with asymmetric boundary

conditions, this diagram consists of a series of evenly spaced peaks and troughs with the peaks occurring at the odd multiples of ω_{th} and the troughs occurring at the even multiples of ω_{th}. While the location of the resonance (peaks) and anti-resonance (troughs) points on the frequency axis is fixed by the system characteristics, the response magnitudes at these frequencies are affected by the position of the measuring point (Muto *et al.* 1980). Figure 4 shows the magnitude of various peaks and troughs in the FRD as a function of the measurement position along the pipe for the system shown in Figure 1. Each series in Figure 4 describes the magnitude of response from a particular harmonic frequency, and each changes significantly with the measuring position. The shape of the FRD at any position in the pipeline can be derived from the relative magnitude of the harmonics at that position. The FRD at 742 m and 2000 m along the pipe are shown as insets in the figure.

The peaks and troughs of all harmonics converge at the extremities of the pipeline. The FRD produced from the downstream end of the pipeline is particularly important as it displays equal magnitude peaks and troughs as a result of this convergence. From Figure 4, the frequency response for all harmonic peaks are also at a maximum at the downstream boundary, resulting in stronger signals and a subsequent higher signal to noise ratio (Lee *et al.* 2002a). The importance of this measurement position becomes apparent when the impact of a leak on the FRD is considered.

The impact of a leak on the FRD measured at the end of the pipe is shown in Figure 5. The figure indicates that a leak causes non-uniform damping of the resonance peaks in the FRD. This finding is also confirmed in Ferrante *et al.* (2001) and Lee *et al.* (2002a, 2002b).

The importance of the measurement position in relation to leak detection can be seen in Figure 5. When the response is measured at the excitation boundary of the pipeline, the FRD of an intact pipeline (no leak) consists of a series of equally spaced peaks of equal magnitude. The presence of a leak results in a deviation of the FRD from this known pattern and clearly indicates the presence of a leak prior to the application of any leak analysis techniques. The impact of a leak on the frequency response measured at any other position in the pipeline does not result in such a clear indication of deviation from the non-leaking situation. A simple data pre-processor that measures the magnitude of the response at harmonic frequencies can be used as a method of quick leak detection within the pipeline when the output is measured at the excitation boundary of the system.

INVERSE RESONANCE TECHNIQUE

As indicated in Figure 5, a leak in a single pipeline can lead to a change in the shape of the FRD, caused by the frequency-dependent damping of components in the transient signal. Inverse fitting minimizes the sum of the difference squared between measured and modeled frequency response functions by varying the value of leak size (C_dA_L) and leak position (x_L) within the model. This method is similar to the inverse transient method in Liggett and Chen (1994). The objective function is given by the least-squares criterion

$$E = \sum_{j=1}^{M} \left[h_j^m - h_j \right]^2 \tag{16}$$

where E is the objective function value, h_j^m and h_j are the measured and calculated amplitude responses at the j^{th} frequency respectively, and M = number of measurement points.

The minimization algorithm used for the results in this paper is shuffled complex evolution (SCE) algorithm (Duan *et al*. 1993). The SCE algorithm performs a global search based on the simplex method and does not require the use of local gradient information. To illustrate the impact of measuring position and selection of calibration points on this process, two examples are presented. The first shows the inverse calibration at an arbitrary internal point within the pipeline using the response at 100 different frequencies. The second, using inverse calibration at the end of the pipeline, resulted in significant simplification of the technique such that only harmonic responses were needed to perform the calibration.

Results for an Example Problem

The results from the application of the inverse resonance method for a FRD measured at a point 800 m from the upstream boundary is given in Figure 6. The frequency response was extracted from the system shown in Figure 1. The inverse resonance method was performed using “perfect” data generated by the transfer matrix equations. In total, 100 data points from the FRD were used in the calibration. The inverse resonance method was able to determine the exact leak size and position of the leak (C_dA_L =0.0014 m^2 and leak position x_L = 1400 m). Figure 7 shows that the final solution of the inverse resonance method (achieved when the method

converged onto the minimum of the solution space) corresponds to the measured results. The objective function space contains a series of parallel valleys with the true solution at the global minimum. This global minimum, however, is located in a trench of gentle slope, resulting in slow convergence to the solution and low sensitivity to measurement error. This example illustrates the conventional application of inverse transient calibration, where a large number of data points are used in the process. By utilizing properties of the FRD, this technique can be further optimized for speed and efficiency.

The speed of the inverse calibration process can be improved through a change in the measurement position and a reduction in the number of frequency responses used. From the previous section, the shape and magnitude of the FRD were simplified by measuring at the excitation boundary in an open/closed boundary configuration, reducing the impact of system noise on the data through an increase in the response magnitudes (Figure 4). Furthermore, Figure 5 shows that the impact of a leak is most significant at harmonic frequencies (peaks and troughs). The selection of calibration points at the harmonic frequencies results in a reduction of the number of points required in the calibration.

The objective function is reformulated using only information at the harmonics and then normalized by dividing by the first resonant peak,

$$E = \sum_{i=2}^{3} \left(\frac{h^m_{\omega_r i}}{h^m_{\omega_r 1}} - \frac{h_{\omega_r i}}{h_{\omega_r 1}} \right)^2 \tag{17}$$

where, $h_{\omega_r i}$ = the frequency response at the i^{th} harmonic. Dividing the response at the various harmonics by the response at the fundamental frequency forms each ratio.

Eq. (17) is an improvement to Eq. (16) as it allows the calibration process to be independent of the magnitude of input signal. Eq. (17) uses the relative sizes between harmonic peaks and avoids the use of absolute magnitudes within the FRD. As a result, the magnitude of the input no longer affects the calibration process, removing a possible source of systematic error from the analysis.

The use of two ratios—between the second and first harmonic, and between the third and first harmonic—is able to obtain the true solution of the leak size (based on the inverse resonance technique) of C_dA_L =0.0014 m^2 and leak position x_L = 1400m using responses at three different frequencies. The inverse calibration result using this new measurement position and objective function is shown in Figure 8. The objective function (Figure 9) has a well defined minimum, in contrast to Figure 7, thus dramatically increasing the speed of the inverse calibration process.

RESONANCE PEAK-SEQUENCING METHOD FOR LEAK LOCATION

Figures 4 and 8 show that a FRD measured at the excitation boundary of a pipeline system with no leaks yields equal magnitude and evenly spaced harmonic peaks. The impact of a leak on this diagram is frequency dependent and results in an uneven damping of harmonic peaks across the frequency axis. This frequency dependent impact was also shown in Wang *et al.* (2002) and forms the basis of the Wang's transient damping leak detection method. The leak induced damping pattern on the FRD provides valuable information concerning the leak.

This pattern leads to a leak location method in a single pipeline that is based on a rank-sequencing of resonant peaks in the FRD. This method does not require the inverse resonance matching of system responses, but allows the accurate location of a leak through the matching of rank-sequences to entries in a look-up table. To understand the operation of this method, the impact of a leak on the FRD of the system is analyzed.

Figure 10 contains the FRD of the pipeline in Figure 1 for varying leak parameters. Four situations are presented; a non-leaking case, a leak at the 1400 m point with a C_dA_L of 0.00014m^2, a leak at the 700 m point with a C_dA_L of 0.00028m^2 and a leak at the 700 m point with a C_dA_L 0f 0.00014m^2. Ranking the sizes of the resonant peaks in order of magnitude can summarize the shape of the frequency diagram.

Figure 10 shows that the order of the resonant peaks ranked in terms magnitude of the peaks has changed from [2, 5, 3, 1, 4] when the leak is positioned 1400 m from the upper boundary, to [3, 1, 4, 5, 2] when the leak is shifted to 700 m from the upper boundary. The increase in leak size from 0.00014 m^2 to 0.00028 m^2 resulted in

lower magnitudes in all resonant peaks, but the overall shape of the FRD, in particular the relative sizes of the peaks, remains unchanged.

The impact of leak parameters on the resonant peak pattern can be seen in Figure 11 and Figure 12. These figures show the variation of the response magnitude of the first 3 resonant peaks (ω_r= 1.0, 3.0, 5.0), measured at the end of the pipeline in Figure 1, as a function of the leak size and leak location respectively. Figure 11 assumes the leak is fixed at the 1400 m position , while Figure 12 is plotted with a constant leak C_dA_L of 0.00014 m^2. The plot of resonant peak response versus leak size in Figure 11 indicates that the magnitude of response at each harmonic component decreases as the size of the leak increases. While the rate of decrease in the response varies slightly between resonant peaks, the order of the peaks, ranked in terms of magnitude, remains unaffected by the leak size.

In contrast, Figure 12 shows that the relative sizes of the resonant peaks change significantly with the location of the leak. The resonant peak responses are seen to intersect at five leak positions along the pipe, dividing the system into six unequal sections. The intersection of any two resonant peak response curves in Figure 12 indicates exact leak locations. Between each intersection point is a region where the resonant peaks, when ranked in order of magnitude, are arranged in a particular sequence. These sequences remain constant within each region and represent a corresponding shape in the FRD. The shapes of the FRD measured at the lower boundary of the system for leaks located at four different positions in the pipe are inserted in Figure 12. When a leak is present in a particular region of the pipe, the shape of the frequency response diagram follows the rank-sequence for that particular region. The shape of a measured FRD could, therefore, be matched to the shape for a particular region in the pipe and used as a means of locating a leak within the single pipeline system. A summary of these sequences for the first three harmonic peaks are tabulated in Table 2 and can be used as a means of locating a leak within a particular section within the pipe. The rank sequences for intersection points are also shown in Table 2 and correspond to exact leak locations in the pipeline.

To illustrate how sequence coding can be used to locate a leak within a reservoir-pipe-valve system, assume a frequency response curve measured at the valve has the sequence of [$h_{\omega r3}$ (Peak 2) > $h_{\omega r5}$ (Peak 3) >$h_{\omega r1}$(Peak 1)] when the first three resonance peaks are ranked in order of magnitude. From Table 2, the ranking indicates that a leak is located at a distance of 66% -75% of the total pipe length from the upper boundary. Similar rank-order

tables can be generated for higher number of peak harmonics, which would result in a finer discretization of the pipeline, and higher location accuracy. For example, the use of the first six harmonic peaks will result in 32 divisions of the pipe.

The generation of such coding can be performed automatically, where the response of each harmonic component as a function of leak position can be approximated by a sinusoidal function, neglecting the small slope effect of the hydraulic grade line on the response function (Schroeder, 1967),

$$h^*_{\omega_{rn}} = \cos\left(\frac{(2n-1)\pi x}{L}\right) \tag{18}$$

where, $h^*_{\omega_{rn}}$ = the response of the n^{th} harmonic peak component, x is the leak location along the pipe, and L the total length of the pipe.

The intersection of different harmonic response curves and the rank-sequence at each intersect and divided region can be determined from Eq. (18). The resonance peak-sequencing method is best used in conjunction with the inverse resonance method to limit the extent of the search space used in the inverse calibration process. The combination of these two techniques provides a fast and efficient way of detecting leaks in a single pipeline.

GENERATION OF THE FRD UNDER REALISTIC SITUATIONS

The application of the inverse resonance method and the resonance peak-sequencing method hinges upon an accurate evaluation of the FRD. This section illustrates the way in which the FRD can be generated in a short time and under physical constraints.

Chaudhry (1987) proposed a frequency sweeping technique where the system is sequentially excited by a sinusoidal perturbation of the valve of different frequencies. The response at each input is then plotted as a function of the input frequency. The problem with this approach is the long time required to sweep through each frequency, as each frequency requires that the system settle down to steady oscillatory conditions. In

addition, the excitation of a pipeline at the resonance frequencies can also inflict substantial damage to the system (Ogawa *et al.*, 1994).

A faster and more resilient method of analysis is available using linear system theory, as has been demonstrated to characterize input-output relations in a wide range of electrical, biological and mechanical systems (Poussart *et al.* 1977, Akiyama 1986, Watanabe *et al.* 1990, Niederdränk 1997, Heutschi *et al.*1997, Liou 1998). The solutions to the linear equations (Eq. 1) at different frequencies are independent. Therefore, for a wide-band input signal, the ratio between the Fourier spectrum of the output to the input signal gives the characteristic frequency response for the system. The use of a broadband signal as the input can, therefore, provide the whole frequency response function in a single run. Theoretically, the perfect input for such an application is a unit impulse, having a wide frequency spectrum with equal magnitude components (Lynn, 1982). Such a signal, however, requires a large amplitude peak to generate a power spectrum of measurable magnitude and may result in non-linearity effects in the system (Poussart *et al.*, 1977). The accuracy of the measuring devices must also be high to capture accurately the sharp impulse. Small measurement errors lead to significant errors in the frequency spectrum (Niederdränk 1997). An alternative is to use a noise level disturbance with a wide frequency spectrum as the input signal, for example a pseudo-random binary signal (PBRS).

PBRS are signals that randomly shift between a number of set values, for example, a signal that randomly jumps between the values 0 and 1 at a time increment given by Δt. As the characteristics of a random signal may shift between sections of the data, a true estimate of the properties of the signal are obtained only if long sections of the data are used. Alternatively, an averaging technique using the auto-correlation of the time series is often used to provide a valid estimate of the entire PBRS sequence. The auto-correlation process has also been shown to decrease the impact of system noise on the data (Li *et al.*1994, Dallabetta 1996, Liou 1998). In the case of random signals, Eq. (1) becomes,

$$H(\omega) = \frac{R_{IO}(\omega)}{R_{II}(\omega)} \tag{19}$$

where, $H(\omega)$ = the frequency response function, $R_{ab}(\omega)$ = the Fourier transform of the correlation function between "a" and "b" and the subscripts *I* and *O* stand for input and output respectively (Lynn, 1982).

For a PBRS of small time increments between possible state changes, the autocorrelation function of the input approaches a Dirac delta function (Liou, 1998) and the Fourier transform is equal to unity for all frequencies (Lynn, 1982). The frequency response function can then be approximated by the Fourier transform of the cross-correlation function alone,

$$H(\omega) = R_{IO}(\omega) \tag{20}$$

The system in Figure 1 is used to generate the FRD using linear theory by perturbing the valve in a pseudo-random binary fashion instead of sinusoidally. Figure 13, Figure 14 and Figure 15 show the input PBRS $\Delta\tau$ values, the output head measured at the downstream boundary, and the FRD of the system compared to results obtained from the transfer matrix. The system is modeled using the method of characteristics and the time step of the analysis and for the PBRS is set at a value of 0.016 s. A good match is obtained between the two methods.

In practice, wide band signals such as PBRS can be injected into a fluid pipeline through perturbations of existing hydraulic elements such as valves and pumps. The input perturbation pattern must be both measurable and independent of the output pressures. A rotary motor placed on the shaft of an inline valve with an angular displacement transducer will suffice as a valid input signal provided that the valve moves in a pseudo-random fashion.

Conclusion

The shape of the frequency response diagram (FRD) of a pipeline is a direct result of the leak location. It can, therefore, be used as a means of identifying the position of the leak within the system. Two methods of leak detection in a pipeline system are the inverse resonance method and resonance peak-sequencing. The former draws upon existing inverse transient techniques and carries out a parameter estimation process by fitting the measured FRD with the results from a numerical model. Unlike the inverse transient method in the time

domain, the use of the FRD for the fitting allows a substantial reduction in the number of required data points. The use of the first three harmonic responses is adequate in providing a match with the data. The combination of these three points into two ratios in the objective function can remove the impact of source disturbance magnitude from the calibration.

The resonance peak-sequencing method involves the comparison between the shape of the FRD to known shapes generated by leaks at various positions in the pipe. Summarizing the shape of the FRD in a sequence of harmonic peaks, ranked in order of magnitude, can provide the means through which this comparison is carried out.

Both methods provide accurate information concerning the leak. The resonance peak-sequencing method is a fast and efficient method of locating a leak within the pipeline and should be used in conjunction with the inverse resonance method to limit the size of the search space.

Finally, the use of pseudo-random binary signals and linear systems theory can lead to a fast estimation of the frequency response curve, making the use of frequency response techniques in leak detection in field situations a distinct possibility.

NOTATION

a wave speed

A area of pipeline

A_0 area of leak orifice

A_V area of valve orifice

C_d coefficient of discharge for leak orifice

C_V coefficient of discharge for valve orifice

D diameter of pipeline

f Darcy-Weisbach friction factor

g gravitational acceleration

H hydraulic grade line

h magnitude of head perturbation

h^* complex hydraulic grade line perturbation

H_0 steady state hydraulic grade line, center of perturbation

H_L head at the leak orifice

H_{L0} steady state head at the leak

H_{V0} steady state head loss across the valve

i imaginary unit, $\sqrt{-1}$

L total length of pipeline

L_1, L_2 lengths of pipe subdivided by the leak

Q discharge

q magnitude of discharge perturbation

q^* complex discharge perturbation

Q_0 steady state discharge, centre of perturbation

Q_L discharge out of the leak orifice.

Q_{L0} steady state flow out of the leak

Q_{V0} steady state flow through the valve

R frictional resistance term

t time

x distance along pipe

Z	characteristic impedance
$\Delta\tau$	magnitude of the dimensionless valve aperture perturbation
μ	propagation constant
τ	dimensionless valve aperture size
τ_0	mean dimensionless valve aperture size, center of perturbation
υ	kinematic viscosity
ω	frequency
ω_{th}	fundamental frequency of system

REFERENCES

Akiyama, T. (1986). “Pressure estimation from oscillatory signals obtained through BWR’s instrument lines.” *Journal of Dynamic Systems, Measurement and Control.* **108** (3), pp. 80 – 85.

Alaskan Department of Environmental Conservation (2001), “Technical review of leak detection technologies” *Crude Oil Transmission Pipelines*.Vol.(**I**).

American Water Works Association (1987), “Leaks in water distribution systems: a technical/economic overview”, *AWWA*, Denver.

Antonopoulous-Domis, M. (1980). “Frequency dependence of acoustic resonances on blockage position in a fast reactor subassembly wrapper.” *Journal of Sound and Vibration*, **72**(4), pp. 443-450.

Black, P. (1992). “A review of pipeline leak detection technology.” *Pipeline Systems*, B. Coulbeck and E. Evans, eds., Kluwer Academic Publishers, pp. 287-297.

Brunone, B. (1999). “Transient test-based technique for leak detection in outfall pipes,” *Journal of Water Resources Planning and Management*, ASCE, **125**(5), Sept/Oct, pp. 302-306.

Chaudhry, M. H. (1987). *Applied Hydraulic Transients.* Van Nostrand Reinhold Company Inc, New York.

Chaudhry, M.H. (1970). “Resonance in pressurized piping systems.” *Journal of the Hydraulics Division*, ASCE, **96**(HY9), September, 1819-1839.

Covas, D. and Ramos, H. (1999). “Leakage detection in single pipelines using pressure wave behaviour,” *Water Industry System: Modelling and Optimisation Application*, **1**, pp 287-299.

Dallabetta, M. J. (1996). “Using crosscorrelation techniques to determine the impulse response characteristics of linear systems.” *Dissertation submitted to the University of Idaho* in partial fulfillment of the requirements for the Degree of Masters of Science with a Major in Electrical Engineering.

De Salis, M.H.F. and Oldham, D.J. (1999). “Determination of the blockage area function of a finite duct from a single pressure response measurement.” *Journal of Sound and Vibration*, **221**(1), pp 180 – 186

De Salis, M.H.F. and Oldham, D.J. (2001). “The development of a rapid single spectrum method for determining the blockage characteristics of a finite length duct” *Journal of Sound and Vibration*, **243**(4) pp. 625-640

Duan, Q.Y., Gupta, V.K., Sorooshian, S. (1993). “Shuffled Complex Evolution Approach for Effective and Efficient Global Minimization.” *Journal of Optimization Theory and Applications*, **76**(3), March, pp. 501 – 521.

Ferrante, M., Brunone, B., and Rossetti, A.G. (2001) “Harmonic analysis of pressure signal during transients for leak detection in pressurized pipes.” BHR Group. *4th International Conference on Water pipeline system - Managing Pipeline Assets in an Evolving Market.* York, UK: 28-30 March 2001

Fox, J. A. (1989). *Transient flow in pipes, open channels and sewers*. Ellis Horwood Limited, England.

Heutschi, K, Rosenheck, A. (1997). “Outdoor sound propagation measurements using an MLS technique.” *Applied Acoustics*, **51**(1), pp 13 – 32.

Hovey, D., and Farmer, E. (1999). “DOT stats indicate need to refocus pipeline accident prevention.” *Oil and Gas Journal*, **47**(11). pp. 52-57.

Jönsson, L., and Larson, M. (1992). “Leak detection through hydraulic transient analysis.” *Pipeline Systems*, B. Coulbeck and E. Evans, eds., Kluwer Academic Publishers, 273-286.

Lee, P.J., Simpson, A.R., and Lambert, M.F. (2002). “Leak detection in pipelines using transient reflection.” *Submitted to Urban Water Journal*.

Lee, P.J., Vítkovský, J.P., Lambert, M.F., Simpson, A.R., and Liggett, J.A. (2002a). “Leak detection in pipelines using an inverse resonance method.” *2002 Conference on Water Resources Planning & Management*, ASCE, 19-22 May, Virginia, USA. [CDROM]

Lee, P.J., Vítkovský, J.P., Lambert, M.F., Simpson, A.R., and Liggett, J.A. (2002b). “Discussion of - Leak Detection in Pipes by Frequency Response Method Using a Step Excitation”, submitted to *Journal of Hydraulic Research*, IAHR..

Li, H. W., Dallabetta, M. J. and Demuth, H. B. (1994). “Measuring the impulse response of Linear systems using an analog correlator.” *Proceedings – IEEE International Symposium on Circuits and Systems,* **5,** pp. 65 – 68.

Liggett, J.A. and Chen, L.C. (1994). “Inverse transient analysis in pipe network,” *Journal of Hydraulic Engineering*, ASCE, **120**(8), pp. 934-955.

Liou, C. P. (1998). “Pipeline leak detection by impulse response extraction.” *Journal of Fluids Engineering*, ASME, **120**, pp 833 – 838.

Liou, C. P., and Tian, J. (1995). “Leak detection-transient flow simulation approaches.” *Journal of Energy Resources Technology*, ASME, **117**, 243-248.

Lynn, P. (1982). *An introduction to the analysis and processing of signals*. The Macmillan Press Ltd, London and Basingstoke.

Mermelstein, P. (1967). “Determination of the vocal-tract shape from measured format frequencies.” *The Journal of the Acoustical Society of America*, **41**(5), pp 1283 – 1294.

Mpesha, W. (1999). “Leak detection in pipes by frequency response method.” *Dissertation submitted to the University of South Carolina* in partial fulfillment of Doctor of Philosophy, Columbia, SC. USA

Mpesha, W., Chaudhry, M.H., and Gassman, S.L. (2002). “Leak detection in pipes by frequency response method using a step excitation.” *Journal of Hydraulic Research*, IAHR. **40**(1), pp. 55 – 62.

Mpesha, W., Gassman, S.L., and Chaudhry, M.H. (2001). “Leak detection in pipes by frequency response method.” *Journal of Hydraulic Engineering*, ASCE, **127**(2), February, pp. 134-147.

Muto, T. and Kanei, T. (1980). “Resonance and transient response of pressurized complex pipe systems.” *Bulletin of the JSME*, **23** (184), pp. 1610 – 1617.

Nash, G. and Karney, B. (1999). “Efficient inverse transient analysis in series pipe systems.” *Journal of Hydraulic Engineering*, ASCE, **125**(7), July, pp. 761 – 764.

Niederdränk, T. (1997). “Maximum length sequences in non-destructive material testing: application of piezoelectric transducers and effects of time variances.” *Ultrasonics*, **35**, pp 195 – 203.

Ogawa, N., Mikoshiba, T. and Minowas, C. (1994) “Hydraulic effects on a large piping system during strong earthquakes.” *Journal of Pressure Vessel Technology*, ASME, **116,** pp. 161 – 168.

Poussart, D. and Ganguly, U. S. (1977). “Rapid measurement of system kinetics – an instrument for real-time transfer function analysis.” *Proceedings of the IEEE*, **65**(5), pp 741 – 747.

Qunli, W and Fricke, F. (1989). “Estimation of blockage dimensions in a duct using measured eigenfrequency shifts.” *Journal of Sound and Vibration*, **133**(2), pp 289-301.

Qunli, W and Fricke, F. (1991). “ Determination of blockage locations and cross-sectional area in a duct by eigenfrequency shifts”. *Journal of the Acoustical Society of America*, **87**(1), 67-75.

Schroeder, M. R. (1967). “Determination of the geometry of the human vocal tract by acoustic measurements.” *The Journal of the Acoustical Society of America*. **41**(4), Part 2. pp. 1002 – 1010

Scott, D. (1999a). “DOT Mandates API Document for Leak Detection,” *Oil & Gas Journal*, **97**(2), pp. 51-54.

Scott, D. (1999b). “PC-Based SCADA installed on Russian crude-oil system,” *Oil & Gas Journal*, **97**(2), pp. 56-57.

Simpson, A., Vítkovský, J., and Lambert, M. (2000). “Transients for calibration of pipe roughnesses using genetic algorithms.” *8th International Conference on Pressure Surges*, The Hague, Netherlands.

Streeter, V. L., Wylie, E. B. (1983). *Fluid mechanics*. McGraw-Hill Book Co., Singapore.

Vítkovský, J.P. (2000). “Experimental verification of inverse transient analysis and unsteady friction,” *Dissertation submitted to the University of Adelaide* in fulfillment of Doctor of Philosophy.

Vítkovský, J.P., Simpson, A.R., Lambert, M.F., and Wang, X.J. (2001). "An Experimental Verification of the Inverse Transient Technique." *6th Conference on Hydraulics in Civil Engineering*, I.E.Aust., 28-30 November, Hobart, Australia, pp. 373-380.

Vítkovský, J.P., and Simpson, A.R. (1997). “Calibration and leak detection in pipe networks using inverse transient analysis and genetic algorithms,” *Research Report* No. R157, August, Department of Civil and Environmental Engineering, University of Adelaide, Australia.

Vítkovský, J.P., and Simpson, A.R. and Lambert, M.F. (1999). “Leak detection and calibration of water distribution system using transient and genetic algorithms,” *Water Distribution System Conference, Division of Water Resource Planning and Management*, ASCE, Tempe, Arizona, 7-9 June.

Wang, X.J., Lambert, M.F., Simpson, A.R., Liggett, J.A., and Vítkovský, J.P. (2002). “Leak Detection in Pipeline Systems Using the Damping of Fluid Transients.” *Journal of Hydraulic Engineering*, ASCE, 128(7), July, 697-711.

Watanabe, K., Koyama, H. (1990). “Location and estimation of a pipeline leak.” *Electrical engineering in Japan*, **110**(7), pp. 92 – 100.

Wylie, E. B., Streeter, V. L. and Suo, L. (1993). *Fluid transients in systems*. Prentice Hall, Englewood Cliffs, New Jersey, USA.

Zielke, W., Rösl, G. (1971). “Resonance in pressurized piping systems – discussion.” *Journal of the Hydraulics Division*, ASCE, **97**(HY7), pp. 1141 – 1146.

Zielke, W., Wylie, E. B., Keller, R. B. (1969). “Forced and self-excited oscillations in propellant lines.” *Journal of Basic Engineering.* (12), pp. 671 – 677.

Table 1 – System parameters for pipeline example in Figure 1

Parameter	**Value**
L_1	1400 m
L_2	600 m
D_1	0.30 m
D_2	0.30 m
H_1	50.0 m
H_2	20.0 m
a_1	1200 m/s
a_2	1200 m/s
f_1	0.020
f_2	0.022
$\Delta\tau$	0.1
Q_0	0.0153 m^3/s
$C_d A_0$ / A_{pipe}	0.2%

Table 2 - Peak ranking Sequence and corresponsing leak position

PEAK RANKING	LEAK LOCATION RANGE (% OF PIPE LENGTH FROM UPPER BOUNDARY)
$h^*_{\omega r1} > h^*_{\omega r3} > h^*_{\omega r5}$	0% - 25%
$h^*_{\omega r1} > \left(h^*_{\omega r3} = h^*_{\omega r5}\right)$	25%
$h^*_{\omega r1} > h^*_{\omega r5} > h^*_{\omega r3}$	25% - 33%
$\left(h^*_{\omega r5} = h^*_{\omega r1}\right) > h^*_{\omega r3}$	33%
$h^*_{\omega r5} > h^*_{\omega r1} > h^*_{\omega r3}$	33% - 50%
$h^*_{\omega r5} = h^*_{\omega r1} = h^*_{\omega r3}$	50% (or 0% or 100%)
$h^*_{\omega r3} > h^*_{\omega r1} > h^*_{\omega r5}$	50% - 66%
$h^*_{\omega r3} > \left(h^*_{\omega r5} = h^*_{\omega r1}\right)$	66%
$h^*_{\omega r3} > h^*_{\omega r5} > h^*_{\omega r1}$	66%-75%
$\left(h^*_{\omega r5} = h^*_{\omega r3}\right) > h^*_{\omega r1}$	75%
$h^*_{\omega r5} > h^*_{\omega r3} > h^*_{\omega r1}$	75% - 100%

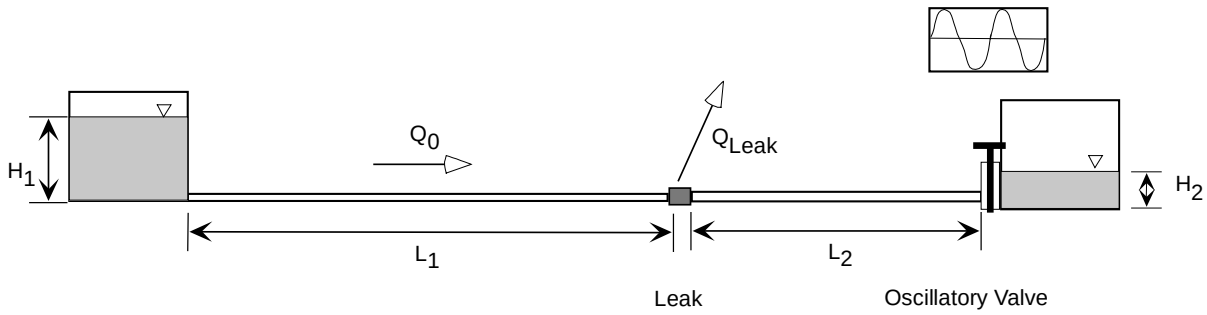

Figure 1 – Single pipeline used for proposed resonance leak detection method

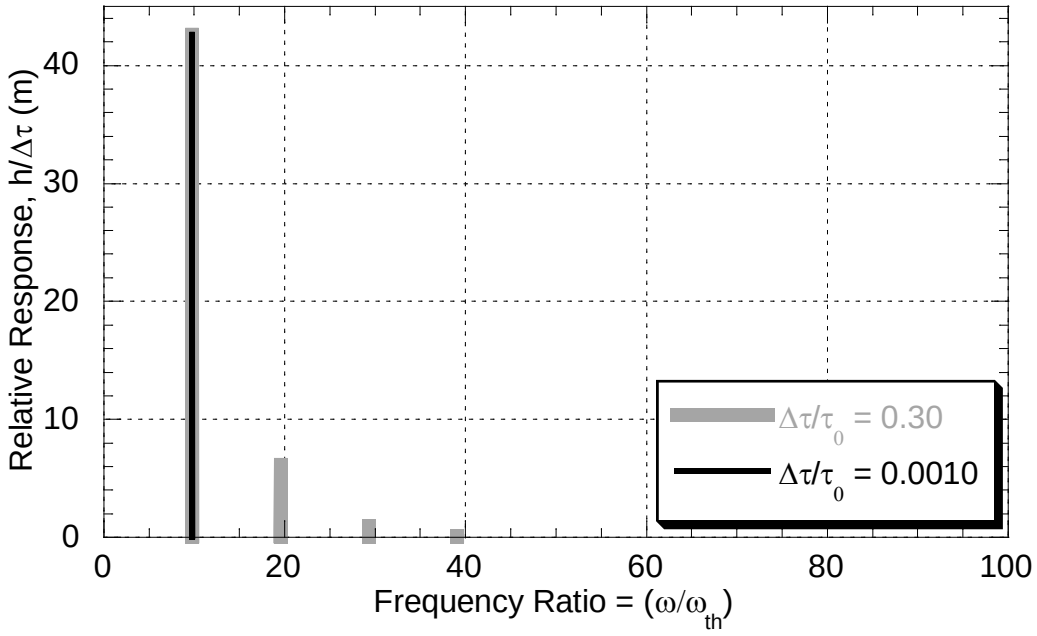

Figure 2 - Fourier decomposition of time series transient traces from method of characteristics for a reservoir-pipe-valve system with no leak and for forcing functions of two different magnitudes.

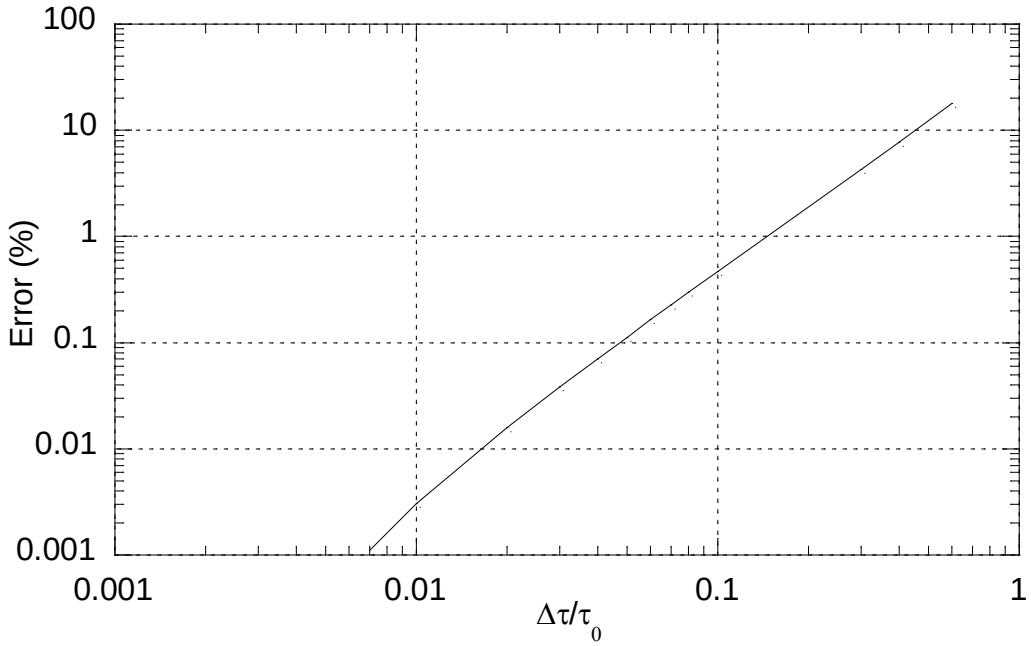

Figure 3 – Percentage error at $\omega/\omega_{th} = 1.0$ as a function of the magnitude of valve perturbation

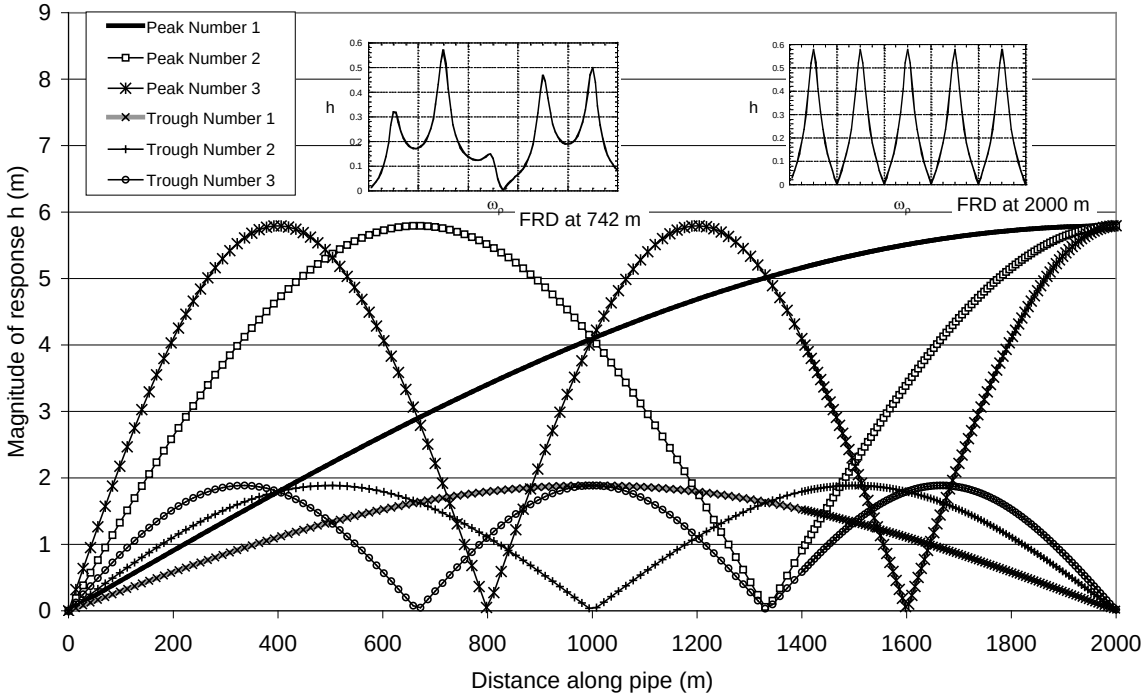

Figure 4 – Response of major harmonic frequencies as measurement position is changed along the non leaking pipeline of Figure 1

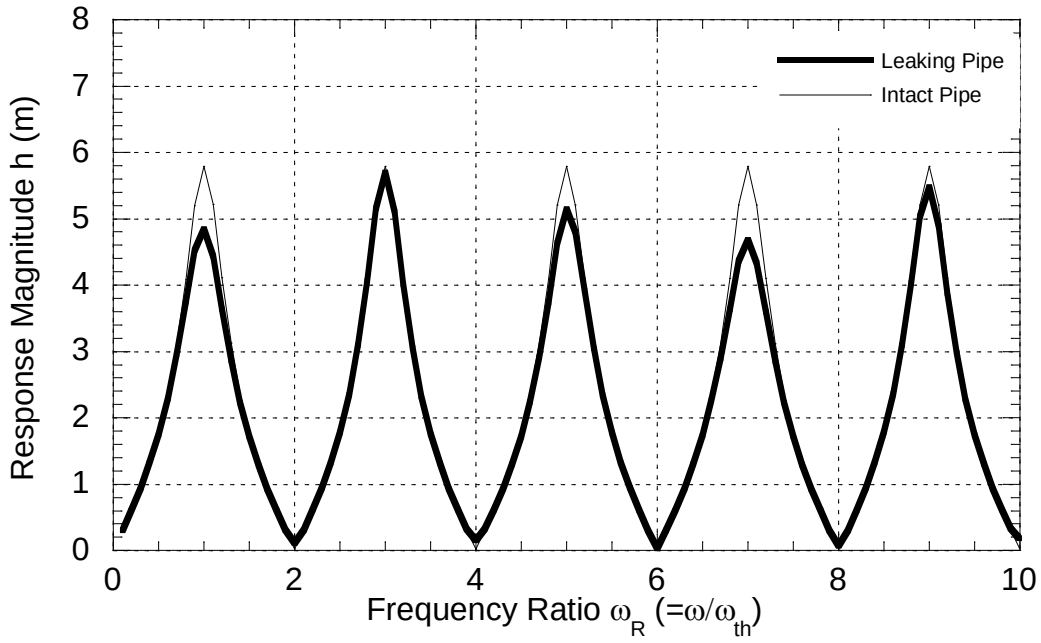

Figure 5 – Frequency response from the leaking and intact pipeline of Figure 1

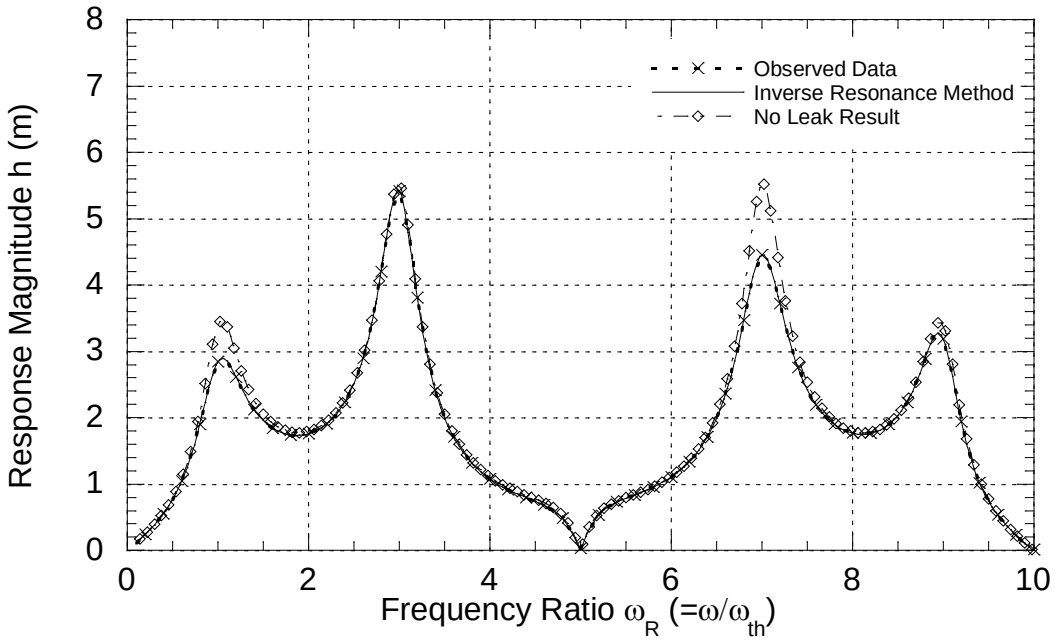

Figure 6 – Inverse resonance fitting for the frequency response measured at a location 800 m from the upstream boundary

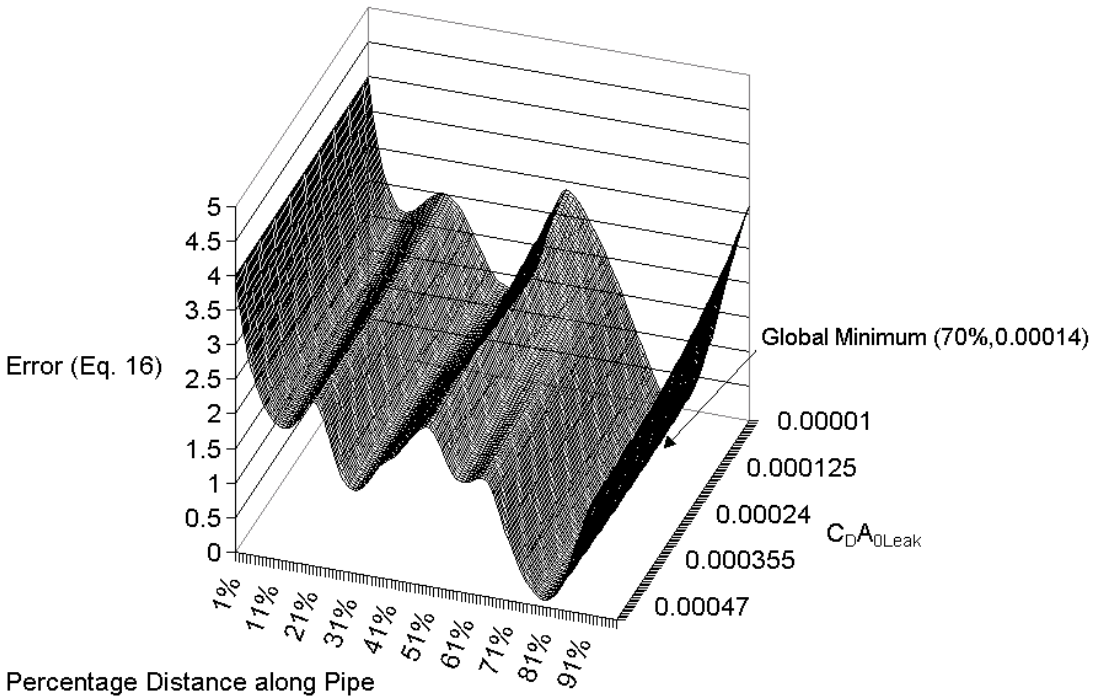

Figure 7 – Error surface for the inverse resonance fitting for the frequency response measured at a location 800 m from the upstream boundary

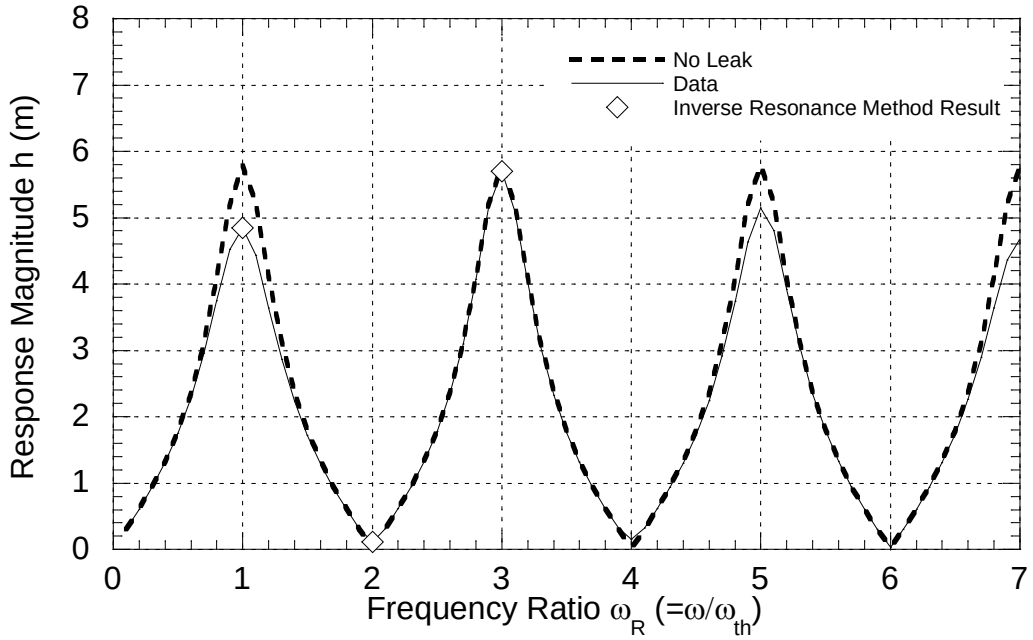

Figure 8 - Inverse resonance fitting for the frequency response measured at the downstream end point using two resonance peak ratios

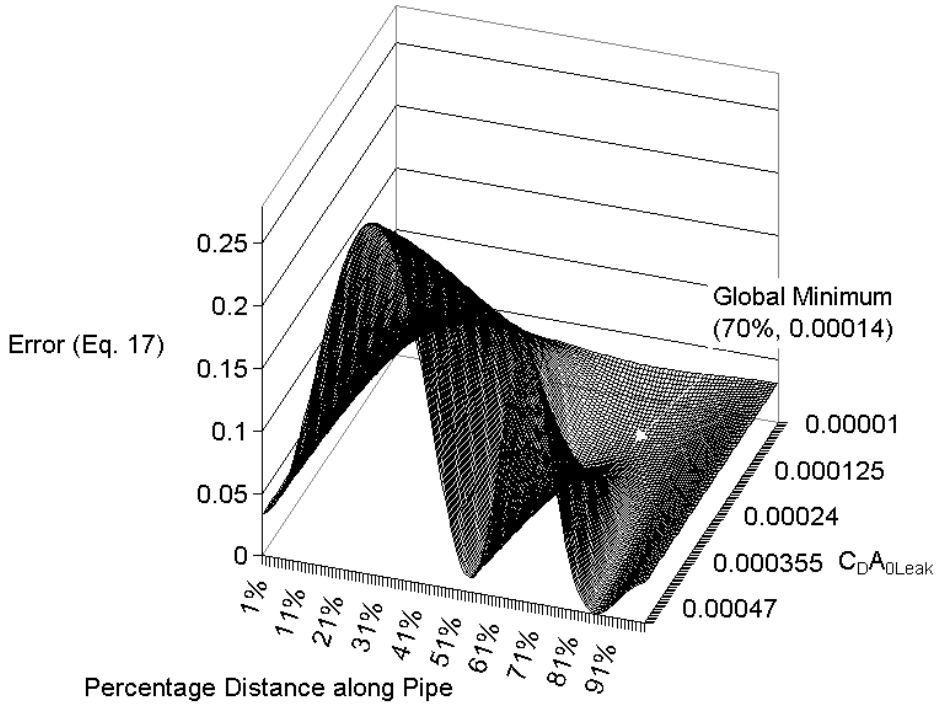

Figure 9 – Error surface of the inverse resonance fitting measured at the downstream end point using two resonance peak ratios

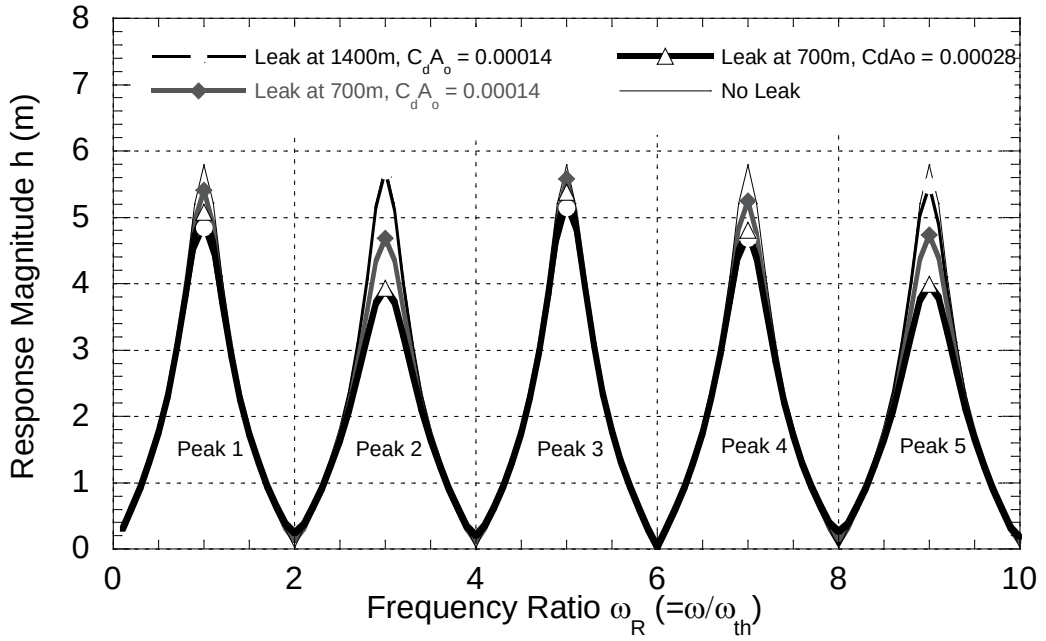

Figure 10 – Impact of changing leak size and position on the frequency response diagram

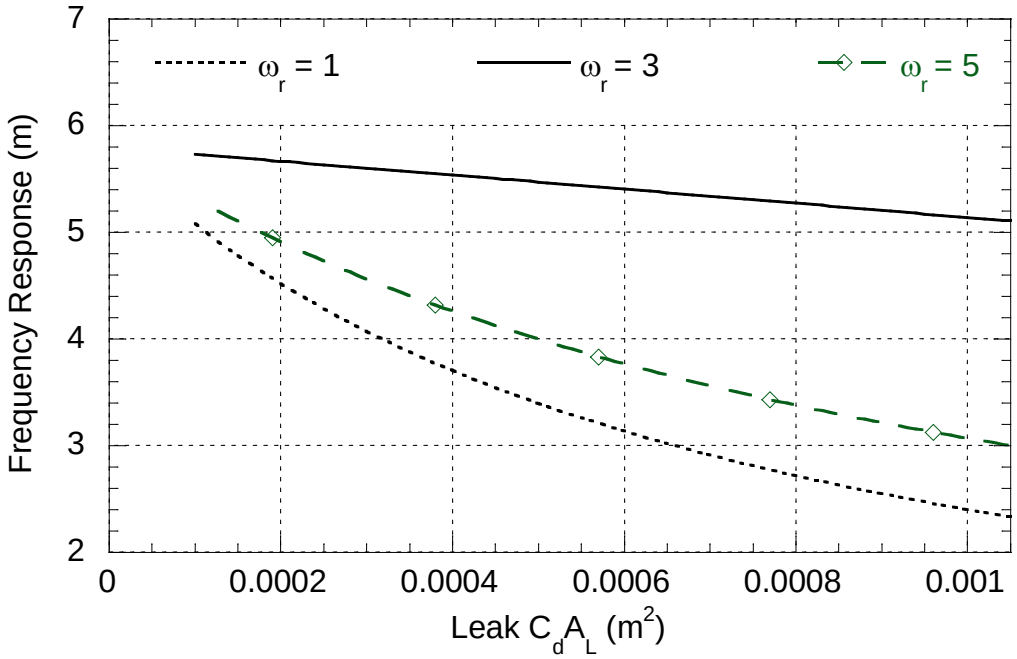

Figure 11 – Impact of leak size on the frequency response of the first 3 harmonic peaks

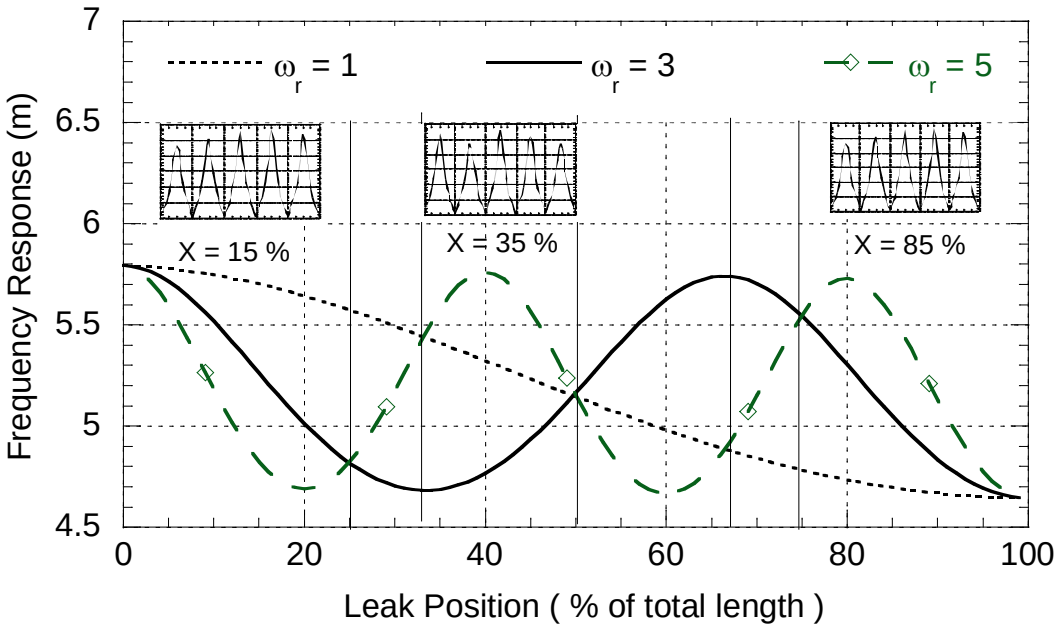

Figure 12 – Impact of leak position on the frequency response of the first 3 harmonic peaks

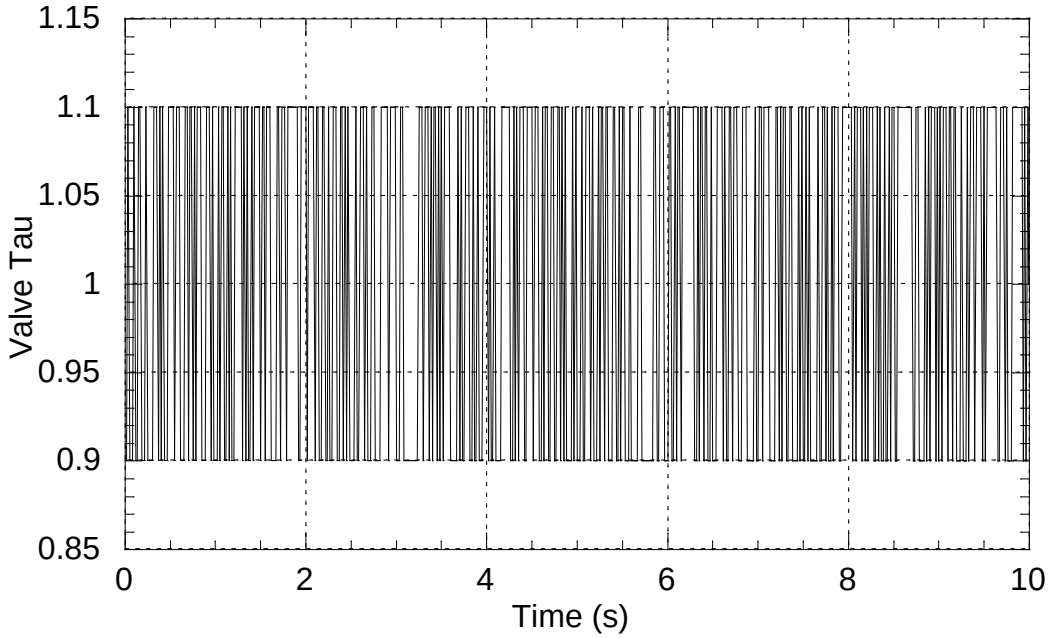

Figure 13 – Input τ fluctuation at the valve based on a broad band pseudo-random binary signal with a time step of 0.016 s in the system of Figure 1

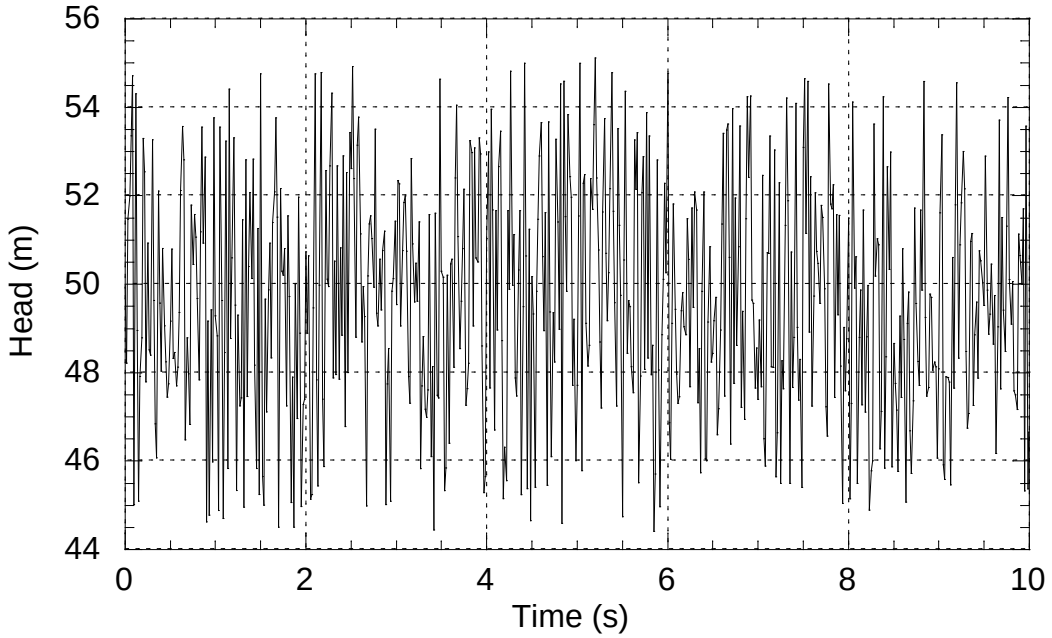

Figure 14 – Output measured head upstream of the valve based on a broad band pseudo-random binary signal with a time step of 0.016 s in the system of Figure 1

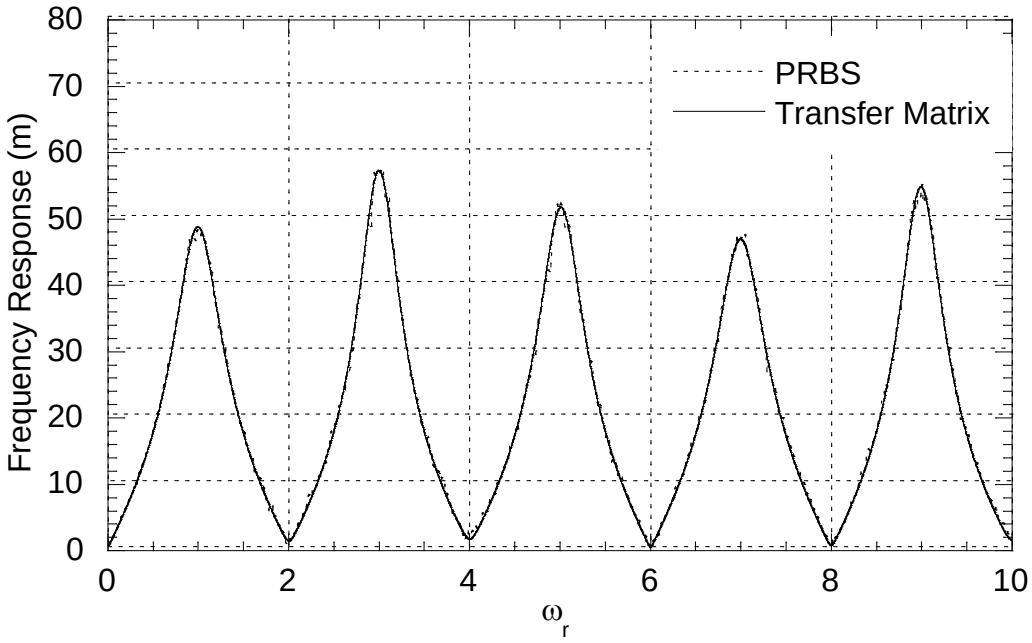

Figure 15 – Comparison of transfer function from transfer matrix and linear theory